A Novel Immense Configurations of Boost Converter for Renewable Energy Application

Pandav Kiran Maroti*, Sanjeevikumar Padmanaban**, Frede Blaabjerg†, Dan Ionel††, Patrick Wheeler†††

**Dept. of Electrical and Electronics Engg.,Marathwada Institute of Technology, India. kiranpandav88@yahoo.co.in,*
***Dept. of Energy Technology, Aalborg University, Esbjerg, Denmark. san@et.aau.dk,*
†Center of Reliable Power Electronics (CORPE), Dept. of Energy Technology, Aalborg University, Denmark. fbl@et.aau.dk
††Power & Energy Institute of Kentucky (PEIK), SPARK Laboratory, Dept. of Electrical and Computer Engg., University of Kentucky, United States. Dan.ionel@uky.edu.
†††Power Electronics, Machines and Control Group (PEMC), Dept. of Electrical & Electronics Engg., Nottingham University, United Kingdom. pat.wheeler@nottingham.ac.uk

Keywords: High gain dc-dc converter, modified boost converter, voltage lift switched inductor, photovoltaic application.

Abstract

A three immense configurations of boost converter for renewable energy application is presented in the paper. The Voltage Lift Switched Inductor (VLSI) structure is pledge to extra high voltage conversion. The proposed work represent the modified high voltage conversion boost converter (MBC) and its three configuration with VLSI module namely, Modified Boost Converter with XL Configuration (MBC_{VLSI}-XL), Modified Boost Converter with LY configuration (MBC_{VLSI}-LY) and Modified Boost Converter with XY configuration (MBC_{VLSI}-XY). The advantage of proposed converter configurations are-(i) immense voltage conversion ratio for high voltage and low current renewable energy applications, (ii) single switch topologies, (iii) input inductor to avoid reverse current flow from load to source. The detail mathematical analysis of proposed configurations are done with and without considering the internal voltage drop across the circuit components. The comparative investigation is carried out with existed high voltage conversion ratio topologies. The Matlab simulation results validates the working of proposed MBC configurations.

1 Introduction

Now a days, industrial, transportation and home appliances are utilizing renewable energy sources such as solar, wind instead of conventional energy sources due to various limitation of them [1,2]. Among the renewable energy sources, photovoltaic is getting more attraction due to its advantages features. A DC-DC converter is a key intermediate stage between energy conversion process from solar PV (low voltage) to grid or electric vehicle or DC electrical appliances [3].

In last decade, various DC-DC converters are introduced which are having high voltage conversion ratio capability. The high voltage at output is achieved either by utilizing transformer, coupled inductor, voltage multiple unit or voltage boosting technique. An isolated high voltage conversion ratio boost converter presented in [4] which achieve high gain by adopting the transformer in the circuit. The drawback of isolated converter is bulky transformer which increases the circuit size and affects the overall efficiency of the converter. In [5,6], a non-isolated high gain DC-DC boost converters are presented which achieves required high voltage by adopting coupled inductor and switched capacitor techniques. The advantage of presented topology is single switch which achieve zero current switching to reduce the conduction losses. A new high gain boost converter is proposed in [7] which shows reduced output voltage ripple content, high voltage conversion ratio and reduced voltage stress across boost switch accomplish by utilizing clamping circuit. A voltage conversion ratio of conventional boost converter is increased by adopting multistage switched inductor technique (SIBC) [8]. One stage of stack, increases overall voltage conversion ratio by addition of D/(1-D). In [9], a transformer less high gain DC-DC converter is presented. A Quadratic Boost Converter (QBC) is combination of two boost converter connected in series to attain high voltage conversion ratio [10].
By considering advantage of QBC over conventional boost converter, voltage conversion ratio of QBC is increase by

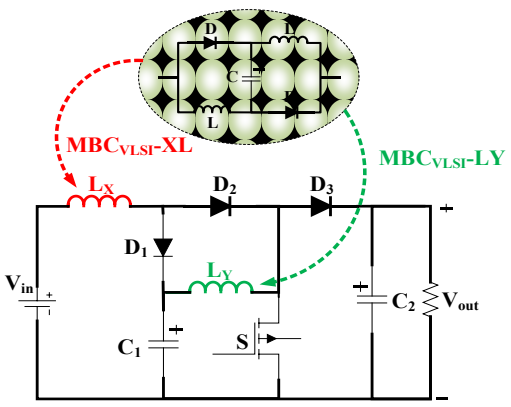

Fig. 1 Modified boost converter with voltage lift switched inductor module

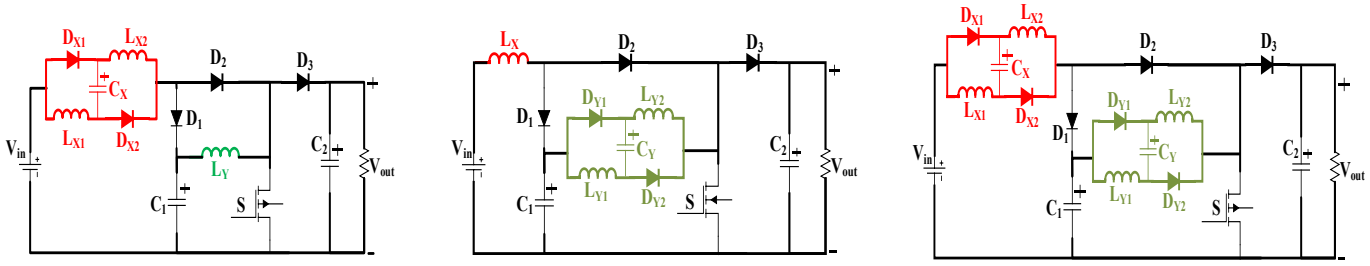

(a) (b) (c)

Fig. 2 Modified boost converter with VLSI module at (a) L_X position, (b) L_Y position and (c) L_X and L_Y position

implementing feature of voltage multiplier unit and voltage lift technique. A QBC with voltage multiplier unit at output side and coupled inductor at input side is added to achieve high gain and to reduce the ripple content of input current respectively [11,12].

A Switched Inductor (SI) module is adopted in QBC to achieve high gain [13]. One stage of SI module increase overall voltage conversion ratio by addition of D/(1-D). By applying concept of QBC, a Modified SEPIC Converter (MSC) is derived by cascading of boost and SEPIC converter with single controlled switch [14]. The voltage conversion ratio of MSC is improve by implementing SI module [15]. VThe above discussed topologies are having high voltage conversion ratio but with high voltage stress across controlled switch which decreases the overall efficiency. In [16], a modified SEPIC boost converter with voltage multiplier unit is presented. The presented converter have high voltage conversion ratio with voltage stress across switch is one third of output voltage. By considering advantage and disadvantage of discussed high voltage gain converter, a new family of high voltage conversion ratio is presented in next section.

2 Modified Boost Converter with VLSI Module

The proposed converter configurations are an extension work of Modified Boost Converter (MBC) and Modified Boost Converter with SI module (MBC_{SI}). The MBC is a combination of two conventional boost converter. The MBCSI is derived by replacing inductor of MBC by SI module which increase the overall gain by (1+D) times of conventional boost converter in each configurations. The MBC_{VLSI} is derived by replacing inductor of MBC by VLSI module as shown in Fig. 1 which increase the overall voltage conversion ratio by four times of conventional boost converter in MBC_{VLSI}-XY configuration. One VLSI module increase the overall voltage conversion ratio by addition of (1/1-D) in each boost converter. According to the position of VLSI module on the place of inductor L_X and L_Y, the MBC is classified into three configuration as MBC_{VLSI}-XL by replacing inductor L_X, MBC_{VLSI}-LY by replacing inductor L_Y and MBC_{VLSI}-XY by replacing both inductors L_X and L_Y by VLSI modules as shown in Fig. 2 (a)-(c). The advantage of proposed configurations of MBC are, 1) single switch topology, 2) extremely high voltage conversion ratio with minimum number of active and passive components, 3) input inductor to avoid reverse current flow from load to source side. The number of active and passive components required for each configuration is articulated in Table 1.

Modified boost converter with VLSI module						
Modified Boost Converter		Component			Voltage conversion ratio	
		L	C	D	V_{C1}/V_{in}	V_0/V_{in}
VLSI Module	XL	3	3	5	2/(1-D)	$2/(1-D)^2$
	LY	3	3	5	1/(1-D)	$2/(1-D)^2$
	XY	4	4	7	2/(1-D)	$4/(1-D)^2$

Table 1: Number of components and voltage conversion ratio of proposed converter Configurations

The working of proposed converter is same as MBC except VLSI module. In VLSI module, both inductor and capacitor are charges equal to V_{in} through diodes during conducting state of switch. Two inductors and capacitor are discharge in series with input supply in non-conducting state of switch to boost the output voltage. The working operation of three configuration is nearly same except the at the VLSI module position. For simplicity, working of MBC_{VLSI}-XY configuration is explained.

2.1 Working of MBC_{VLSI}-XY configuration

The operation of MBC_{VLSI}-XY configuration is separated into two part as switch ON mode and switch OFF mode as discuss in detail in following sub section.

1) Switch ON mode

During ON state of switch S, two inductors (L_{X1} and L_{X2}) are energies up to input supply V_{in} with help of diodes D_{X1} and D_{X2} respectively and along with diode D_2 and switch S. Similarly, capacitor C_X is charges from V_{in} via diodes D_{X1}, D_{X2}, D_2 and switch S as shown in Fig. 3(a). In the same way, two inductors (L_{Y1} and L_{Y2}) are energies up to capacitor C_1 via diodes D_{Y1} and D_{Y2} respectively along with switch S. Capacitor C_Y is charges up to V_{C1} via diodes D_{Y1} and D_{Y2} respectively along with switch S. Diode D_3 is in reverse bias due capacitor C_2. During switch ON mode, output is equals to voltage across capacitor C_2.

2) Switch OFF mode

During OFF state of switch S, charged inductors L_{X1}, L_{X2} and capacitor C_X transfer the energy to capacitor C_1 along with input supply V_{in} via diode D_1 as shown in Fig. 3(b). Similarly, capacitor C_2 is charges from inductors L_{Y1}, L_{Y2} and capacitor C_Y along with input supply V_{in}, inductors L_{X1}, L_{X2} and capacitor C_X via diode D_3. In OFF mode, diode D_2 is in reverse bias state.

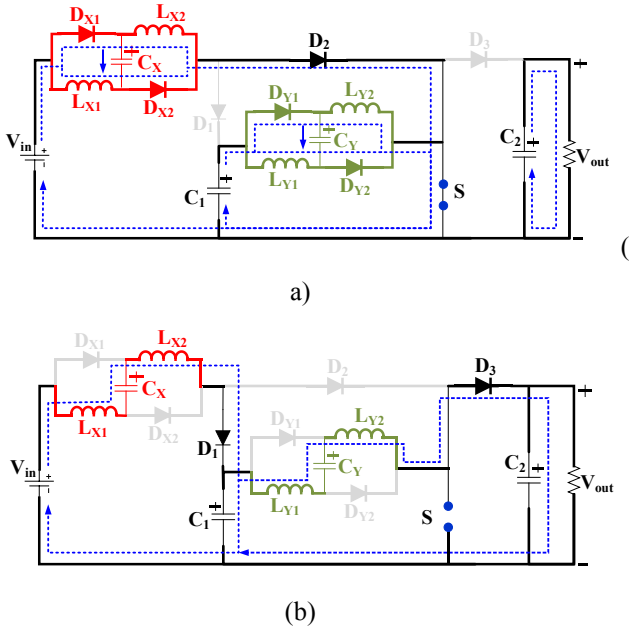

Fig. 3 Working of MBC_{VLSI}-XY configuration in (a) switch ON mode and (b) switch OFF mode

3 Analysis of Voltage Conversion Ratio of Proposed MBC Configurations with VLSI Module

This section deals with detail analysis of voltage conversion ratio of MBC_{VLSI}-XL, LY and XY configuration in continuous conduction mode. The analysis is done with and without considering the internal voltage drop of circuit components.

1) MBC_{VLSI}-LL Configuration

The voltage conversion ratio of MBC_{VLSI}-LL configuration is expressed as [13],

$$V_0 = \frac{1}{(1-D)^2} V_{in} \tag{1}$$

2) MBC_{VLSI}-XL Configuration

Steady state equations of circuit during CCM are

$$\left.\begin{aligned} V_{LX1} &= V_{LX2} = V_{in} - 2V_{d(L)} - V_{d(D)} - V_{d(S)} \\ V_{CX} &= V_{in} - 2V_{d(L)} - V_{d(D)} - V_{d(S)} \\ V_{LY} &= V_{C1} - V_{d(L)} - V_{d(S)} \end{aligned}\right\} \tag{2}$$

Here $V_{d(L)}$ is voltage drop across each inductor due to its internal resistance. Similarly, $V_{d(D)}$ and $V_{d(S)}$ are voltage drop across uncontrolled diode and controlled switch respectively.

To simplify mathematical analysis, the voltage drop across all device are considered as equal

$$V_{d(L)} = V_{d(D)} = V_{d(S)} = V_d \tag{3}$$

$$\left.\begin{aligned} V_{LX1} &= V_{LX2} = V_{in} - 4V_d \\ V_{CX} &= V_{in} - 4V_d \\ V_{LY} &= V_{C1} - 2V_d \end{aligned}\right\} \text{ON state} \tag{4}$$

$$\left.\begin{aligned} V_{LX1} + V_{LX2} &= V_{in} + V_{CX} - V_{C1} - 3V_d \\ V_{LX} &= \frac{2V_{in} - V_{C1} - 7V_d}{2} \\ V_{LY} &= V_{C1} - V_0 - 2V_d \end{aligned}\right\} \text{OFF state} \tag{5}$$

By volt second balance law for inductor L_X

$$\int_0^{DTs} (V_{in} - 4V_d)dt + \int_{DTs}^{Ts} \left(\frac{2V_{in} - V_{C1} - 7V_d}{2}\right)dt = 0 \tag{6}$$

$$V_{C1} = \left(\frac{2}{1-D}\right)V_{in} - \left(\frac{7+D}{1-D}\right)V_d \tag{7}$$

for inductor L_Y

$$\int_0^{DT_S} (V_{C1} - 2V_d)dt + \int_{DT_S}^{T_S} (V_{C1} - V_0 - 2V_d)dt = 0 \tag{8}$$

$$V_0 = \frac{V_{C1}}{(1-D)} - \frac{2V_d}{1-D} \tag{9}$$

by (7)

$$V_0 = \left(\frac{2}{(1-D)^2}\right)V_{in} - \left(\frac{9-D}{(1-D)^2}\right)V_d \tag{10}$$

If internal voltage drop is neglected then voltage conversion ratio is

$$V_0 = \left(\frac{2}{(1-D)^2}\right)V_{in} \tag{11}$$

3) MBC_{VLSI}-LY Configuration

Steady state equations of circuit during CCM are

$$\left.\begin{aligned} V_{LX} &= V_{in} - 3V_d \\ V_{LY1} &= V_{LY2} = V_{C1} - 3V_d \\ V_{CY} &= V_{C1} - 3V_d \end{aligned}\right\} \text{ON state} \tag{12}$$

$$\left.\begin{aligned} V_{LX} &= V_{in} - V_{C1} - 2V_d \\ V_{LY} &= \frac{2V_{C1} - V_0 - 6V_d}{2} \end{aligned}\right\} \text{ OFF state} \quad (13)$$

Parameter	Value
Input voltage	10 V
Output power	250 W
Switching frequency	50 KHz
Duty ratio	70%

Table 2: Simulation parameter and value

By volt second balance law for inductor L_X

$$\int_0^{DT_S} (V_{in} - 3V_d)dt + \int_{DT_S}^{T_S} (V_{in} - V_{C1} - 2V_d)dt = 0 \quad (14)$$

$$V_{C1} = \left(\frac{1}{1-D}\right)V_{in} - \left(\frac{2+D}{1-D}\right)V_d \quad (15)$$

for inductor L_Y

$$\int_0^{DT_S} (V_{C1} - 3V_d)dt - \int_{DT_S}^{T_S} \frac{(2V_{C1} - V_0 - 6V_d)}{2}dt = 0 \quad (16)$$

$$V_0 = \left(\frac{2}{1-D}\right)V_{C1} - \left(\frac{2}{1-D}\right)V_d \quad (17)$$

From (15)

$$V_0 = \frac{2V_{in}}{(1-D)^2} - \frac{6V_d}{(1-D)^2} \quad (18)$$

If internal voltage drop is neglected then voltage conversion ratio is

$$V_0 = \frac{2V_{in}}{(1-D)^2} \quad (19)$$

4) MBC_{VLSI}-XY Configuration

Steady state equations of circuit during CCM are

$$\left.\begin{aligned} V_{LX1} &= V_{LX2} = V_{in} - 4V_d \\ V_{CX} &= V_{in} - 4V_d \\ V_{LY1} &= V_{LY2} = V_{C1} - 3V_d \\ V_{CY} &= V_{C1} - 3V_d \end{aligned}\right\} \text{ ON state} \quad (20)$$

$$\left.\begin{aligned} V_{LX} &= \frac{2V_{in} - V_{C1} - 7V_d}{2} \\ V_{LY} &= \frac{2V_{C1} - V_0 - 6V_d}{2} \end{aligned}\right\} \text{ OFF state} \quad (21)$$

By volt second balance law for inductor L_X

$$\int_0^{DT_S} (V_{in} - 4V_d)dt + \int_{DT_S}^{T_S} \left(\frac{2V_{in} - V_{C1} - 7V_d}{2}\right)dt = 0 \quad (22)$$

$$V_{C1} = \left(\frac{2}{1-D}\right)V_{in} - \left(\frac{7+D}{1-D}\right)V_d \quad (23)$$

for inductor L_Y

$$\int_0^{DT_S} (V_{C1} - 3V_d)dt - \int_{DT_S}^{T_S} \frac{(2V_{C1} - V_0)}{2}dt = 0 \quad (24)$$

$$V_0 = \left(\frac{2}{1-D}\right)V_{C1} - \left(\frac{6}{1-D}\right)V_d \quad (25)$$

From (23)

$$V_0 = \left(\frac{4}{(1-D)^2}\right)V_{in} - \left(\frac{10-4D}{(1-D)^2}\right)V_d \quad (26)$$

If internal voltage drop is neglected then voltage conversion ratio is

$$V_0 = \frac{4V_{in}}{(1-D)^2} \quad (27)$$

4 Result and Discussion

To validates the working operation of proposed three configurations of MBC (MBC_{VLSI}-XL, MBC_{VLSI}-LY, and MBC_{VLSI}-XY), these converter are simulated in Matlab R2016a with resistive load. All three configurations are simulated at high switching frequency to reduce the components size and output waveform ripple content. The simulation parameters and their value for three configurations are tabulated in Table. 2

1) MBC_{VLSI}-XL Configuration

The proposed configuration is simulated with resistive load (197.53 Ω). Proposed converter is two stage converter which give intermediate stage voltage of 66.4 V with fluctuation of 0.45% as presented in Fig. 4(a). Proposed converter provides 221 V at the output with fluctuation of 0.09% as shown in Fig. 4(b). Fig. 4(c) shows the output current waveform with resultant amplitude of 1.112 A with fluctuation of 1.17%. From Figs. 4(b) and (c), proposed configuration work with 245.97 W power and shows efficiency of 98.38%.

2) MBC_{VLSI}-LY Configuration

The proposed configuration is simulated with resistive load (197.53 Ω). The intermediate stage voltage of proposed configuration is 33.1 V with fluctuation of 1.2% as presented in Fig. 5(a). Proposed converter gives 221.6 V at the output with fluctuation of 0.09% as shown in Fig. 5(b). The output current waveform is shown in Fig. 5(c) which shows the resultant current is 1.114 A with fluctuation of 1.5%. From Figs. 5(b) and (c), proposed configuration work with 247.41 W power and shows efficiency of 98.96%.

3) MBC_{VLSI}-XY Configuration

The proposed configuration is simulated with resistive load (788.5 Ω). The intermediate stage voltage of proposed configuration is 65.5 V with fluctuation of 0.6% as presented in Fig. 6(a). Proposed converter gives 443 V at the output with fluctuation of 0.04% as shown in Fig. 6(b). The output

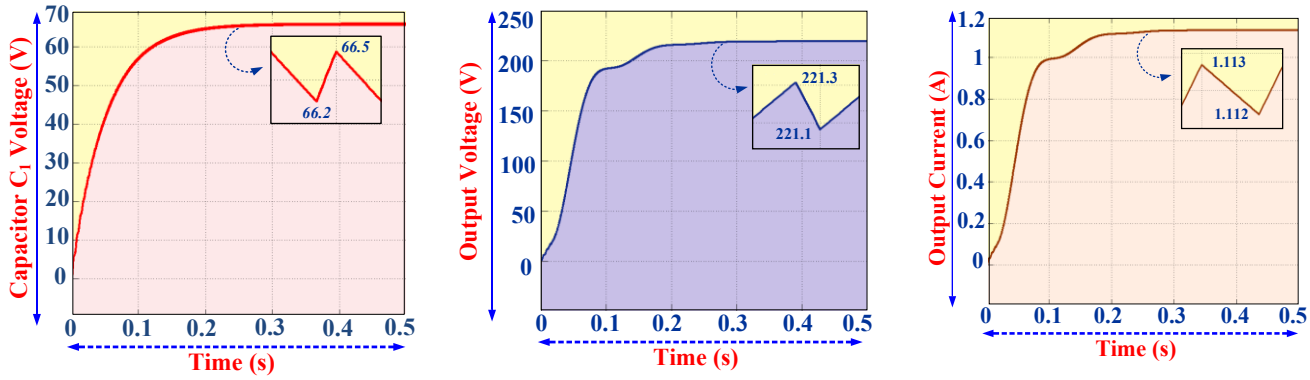

(a) (b) (c)

Fig. 4 Simulation result of MBC_{VLSI}-XL configuration (a) Voltage across capacitor C_1, (b) Output voltage, (c) Output current

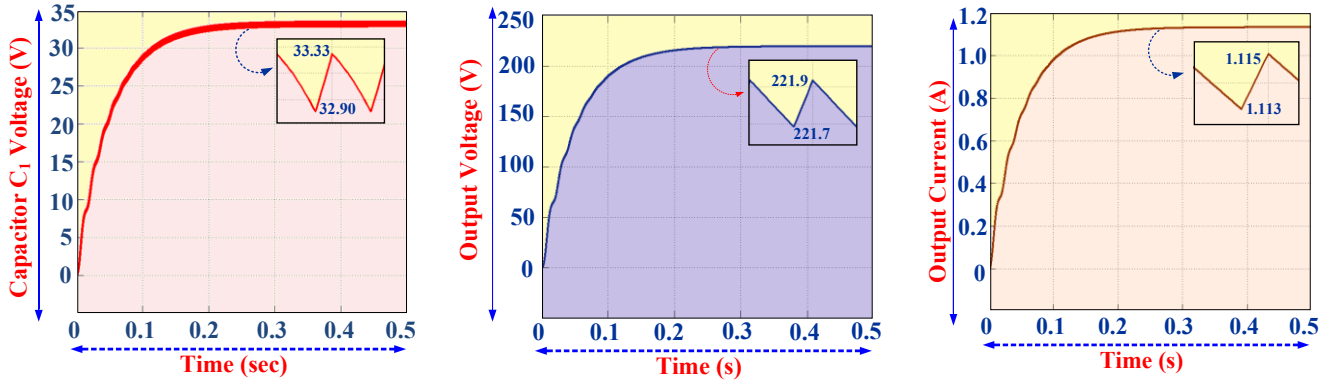

(a) (b) (c)

Fig. 5 Simulation result of MBC_{VLSI}-LY configuration (a) Voltage across capacitor C_1, (b) Output voltage, (c) Output current

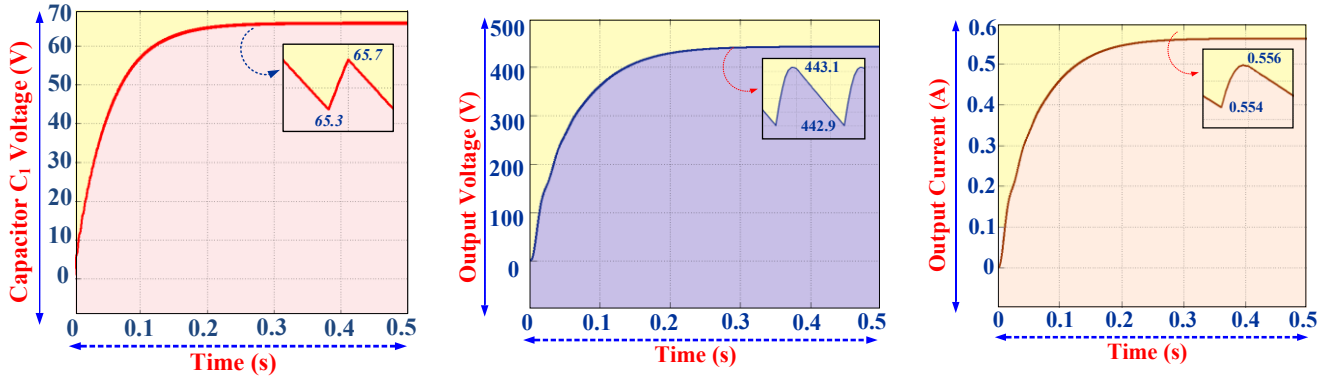

(a) (b) (c)

Fig. 6 Simulation result of MBC_{VLSI}-XY configuration (a) Voltage across capacitor C_1, (b) Output voltage, (c) Output current

current waveform is shown in Fig. 6(c) which shows the resultant current is 0.555 A with fluctuation of 0.36%. From Figs. 6(b) and (c), proposed configuration work with 245.86 W power and shows efficiency of 98.34%. Fig. 7 shows the comparative graph of voltage conversion ratio of three configuration of MBC with VLSI module and cascaded boost converter, conventional boost converter, multistage switched inductor boost converter and MBC with SI module. It shows that, MBC_{VLSI}-XY configuration is having highest voltage conversion ratio among the MBC family, conventional and cascaded boost converter. If internal voltage drop is neglected then, MBC_{VLSI}-XL and MBC_{VLSI}-LY configuration have same voltage conversion ratio.

5 Conclusion

In this paper, the modified boost converter and its three configuration using VLSI module is discussed. The detail comparative analysis of proposed three converter configurations are done with existed high voltage conversion ratio. The detail mathematical analysis of proposed

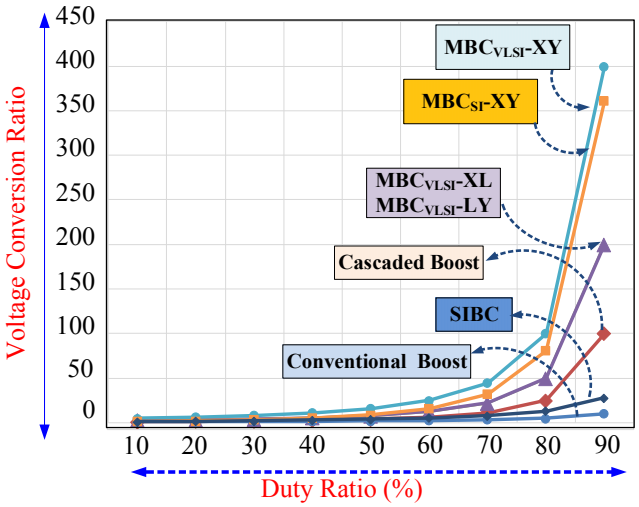

Fig. 7 Graph of voltage conversion ratio of various boost converter configuration with respective duty ratio

configurations are carried out with and without considering the internal voltage drop. The MBC$_{VLSI}$-XY configuration is having highest voltage conversion ratio as well as lower efficiency in among the other two configurations. The MBC$_{VLSI}$-XL and MBC$_{VLSI}$-LY configurations have same voltage conversion ratio in ideal condition and MBC$_{VLSI}$-XL configurations is having lower efficiency as compared to MBC$_{VLSI}$-LY configurations. The detail comparative analysis of three configurations are done with respective their voltage conversion ratio and number of components.

References

[1] F. Blaabjerg, Y. Yang, K. Ma, X. Wang, "Power electronics - the key technology for renewable energy system integration," *Intl. Conf. on Renewable Energy Research and Applications (ICRERA)*, Palermo, pp. 1618-1626, (Nov. 2015).

[2] P. Sanjeevikumar, G. Grandi, P. W. Wheeler, F. Blaabjerg, J. Loncarski, "A simple MPPT algorithm for novel PV power generation system by high output voltage DC-DC boost converter," *IEEE 24th Intl. Symposium on Industrial Electronics (ISIE)*, Buzios, pp. 214-220. (June 2015).

[3] M. Forouzesh, Y. P. Siwakoti, S. A. Gorji, F. Blaabjerg, B. Lehman, "Step-Up DC–DC Converters: A Comprehensive Review of Voltage-Boosting Techniques, Topologies, and Applications," in *IEEE Transactions on Power Electronics*, **vol. 32, no. 12,** pp. 9143-9178, (March 2017).

[4] B. Wu, S. Li, K. M. Smedley, "A New Single-Switch Isolated High-Gain Hybrid Boosting Converter", *IEEE Trans. on Industrial Electronics,* **vol. 63, issue: 8,** pp. 4978-4988, (Aug. 2016).

[5] M. Muhammad, M. Armstrong, M. A. Elgendy, "Analysis and implementation of high-gain non-isolated DC–DC boost converter*", IET Power Electronics*, **vol. 10, issue: 11**, pp. 1241-1249, (sept. 2017).

[6] L. Schmitz, D. C. Martins, R. F. Coelho, "Generalized High Step-Up DC-DC Boost-Based Converter With Gain Cell" *IEEE Trans. on Circuits and Systems I,* **vol. 64, issue: 2,** pp. 480-493, (Feb. 2017).

[7] S. Jain, B. Ritanjali, V. Agarwal, "High-gain boost converter with coupled inductor and switched capacitor for low voltage renewable energy sources", *Power Electronics, Drives and Energy Systems (PEDES),* pp. 1-6. (Dec. 2014).

[8] P. K. Maroti, P. Sanjeevikumar, M. S. Bhaskar, F. Blaabjerg, V. K.Ramachandramurthy, P. Siano, V. Fedák' "Multistage Switched Inductor Boost Converter For Renewable Energy Application", *IEEE Conf. on Energy Conversion, CENCON'17,* pp. 1-6, (Dec. 2017).

[9] J. C. Rosas-Caro, F. Mancilla-David, J. C. Mayo-Maldonado, J. M. Gonzalez-Lopez, H. L. Torres-Espinosa, J. E. Valdez-Resendiz, "A Transformer-less High-Gain Boost Converter With Input Current Ripple Cancelation at a Selectable Duty Cycle", *IEEE Trans. on Industrial Electronics*, **vol. 60, issue: 10,** pp. 4492-4499, (Oct. 2013).

[10] M. A. Al-Saffar, E. H. Ismail, A. J. Sabzali, "High efficiency quadratic boost converter", *Applied Power Electronics Conference and Exposition (APEC), Twenty-Seventh Annual IEEE*, pp. 1245-1252, (Feb. 2012).

[11] J. Leyva-Ramos, R. Mota-Varona, M. G. Ortiz-Lopez, L. H. Diaz-Saldierna, D. Langarica-Cordoba, "Control Strategy of a Quadratic Boost Converter With Voltage Multiplier Cell for High-Voltage Gain", *IEEE Journal of Emerging and Selected Topics in Power Electronics*, **vol. 5, issue: 4,** pp. 1761-1770, (Dec. 2017).

[12] N. Zhang, D. Sutanto, K. M. Muttaqi, B. Zhang, D. Qiu, "High-voltage-gain quadratic boost converter with voltage multiplier", *IET Power Electronics*, **vol. 8, issue: 12,** pp. 2511-2519, (Dec. 2015).

[13] P. K. Maroti, P. Sanjeevikumar, P. Wheeler, F. Blaabjerg, M. Rivera "Modified Boost with Switched Inductor Different Configurational Structures for DC-DC Converter for Renewable Application" *Southern Power Elctronics Conf. (SPEC'17), Chile.* pp.1-6, (Dec 2017).

[14] P. K. Maroti, P.Sanjeevikumar, F. Blaabjerg, V. Fedák, P. Siano, V. K. Ramachandramurthy, "A Novel Switched Inductor Configuration for Modified SEPIC DC-to-DC Converter for Renewable Energy Application", *Conf. on Energy Conversion, CENCON'17*, pp. 1-6, (Dec. 2017).

[15] P. K. Maroti, M. S. Bhaskar, P. Sanjeevikumar, F. Blaabjerg, V. Fedák, "A High Gain Modified SEPIC DC-to-DC Boost Converter for Renewable Energy Application" *3rd IEEE Conference on Energy Conversion, CENCON'17,* pp. 1-6, (Dec. 2017).

[16] P. K. Maroti, P. Sanjeevikumar, F. Blaabjerg, "A Novel Multilevel High Gain Modified SEPIC DC-to-DC Converter for High Voltage and Low Current Applications", *In conf. proc. of IEEE 12th Intl. Conf. on Compatibility, Power Electronics and Power Engineering (CPE-POWERENG'18)*, Doha, Qatar. (April 2018).